

Adaptive Algorithms for Burned Surfaces Automatic Estimation by ATSR-2 Data

Isidoro Piccolini c/o ESA/ESRIN, Directorate of Application, Remote Sensing Exploitation Department, CP 64, Via Galileo Galilei, 00044 Frascati, Italy.
Phone +390694180589. E-mail isidoro.piccolini@esrin.esa.it

Olivier Arino ESA/ESRIN, Directorate of Application, Remote Sensing Exploitation Department, CP 64, Via Galileo Galilei, 00044 Frascati, Italy.
Phone +390694180564. E-mail olivier.arino@esrin.esa.it

Abstract.

The scientific community requests an assessment of fire effects like gas emissions and land cover changes. For so doing, vegetation type and state as well as the extension of the burned surfaces are requested.

This research investigates the best method for estimation of burned area from vegetation fire by ATSR-2 data at regional scale. A set of six different algorithms had been identified and each one produces a map of burned surfaces. All tests are based on an adaptive algorithm.

This allows the minimization of problems that arises from the different atmospheric condition, viewing geometry or vegetation cover type in the scene under analysis. Results are investigated and validated against a set of nine TM images.

1. Introduction

Many vegetation fire events occur around the globe during the year, leading to environmental disasters at different levels.

- At regional scale, with the destruction of vegetation reserve and danger for human activities.
- At global scale, for the atmospheric emissions involved (Lioussé et al., 1997) that contribute to greenhouse effect, thus the raise of the mean temperature of the ground leading to many frightening danger modification for the whole globe (Levine, 1991).

In this context it has been evaluated that the quantity of biomass burning is directly linked to four physical quantities (Seiler e Crutzen, 1980):

$$M=A \cdot B \cdot \alpha \cdot \beta$$

Where:

M is the quantity of biomass burned in gdm/y (grams of dry matter for year);

A is the area in square meter;

B is the total biomass in gdm/m² (grams of dry matter for square meter);

α is the fraction of biomass over the ground with respect to the total biomass *B*;

β is the burning efficiency, the index of the capacity to burn of that biomass.

The last three terms are related to specific ecosystem or vegetation species during the year, whereas the surface extension *A* is a variable that doesn't need "a priori" study and can be evaluated interactively with the proper tools. In order to assess the quantity of biomass burned on the globe many studies have been performed (Pereira et Setzer 1996, Kasischke 1995, Razampifilo 1995). For this task the remote sensing has a significant role, especially if the estimation is requested with frequent updates.

2. Area under study

A squared area of 1000 Km has been selected to develop and test the method. This area has three main characteristics:

- It has a high level of fire activity.
- It contains different types of vegetation.
- It is a fairly flat region which reduces geolocation error of remotely sensed data .

The period of the year chosen for the study corresponds to a phase of high level fire activity within the area. From previous studies (Hao et Liou, 1994) we know that the African continent contributes up to 46% to the total biomass burning in the world. Moreover occurrence of fires in this continent shows a seasonal activity (Arino et Melinotte, 1995) linked to climate variation during the year. In particular, in West and Central Africa the great fire activity occurred from December to March during the dry season. The vegetation data used were evaluated in the context of International Geosphere Biosphere Program (IGBP 1996). The zone under analysis (figure 1) is mainly

composed by savannas in the northern part, with occurrence of grassland and cropland in the extreme north and woody savanna in the southern part, with occurrence of evergreen broadleaf forest in the south. The period of the year identified is January to April 1997, which corresponds to a post-maximum fire activity period.

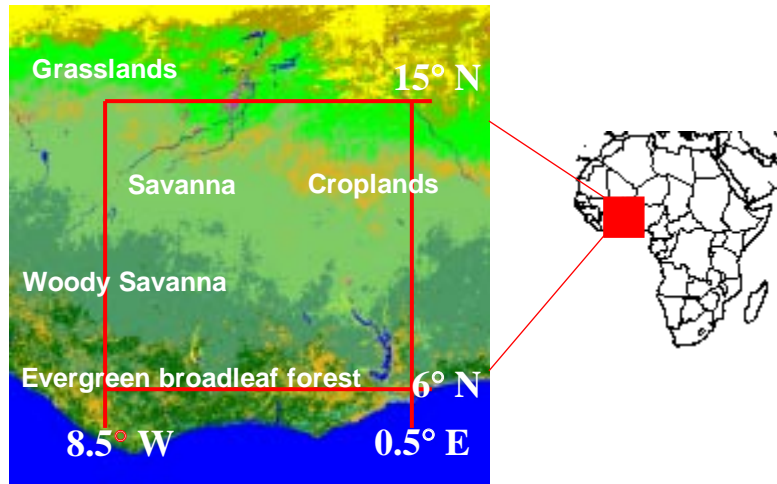


Figure 1. Area under analysis. The different colors show the vegetation types (IGBP 1996), inside the area of 1000Km x 1000 Km in West Africa.

3. ATSR data

The Along Track and Scanning Radiometer (ATSR) is a sensor for environmental monitoring in the visible and infrared wavelength (Stricker et al. 1995). The main task of ATSR-1 (onboard ERS-1 launched 17th July 1991), with its four channel sensors, was high accuracy estimation of sea surface temperature (SST). ATSR-2 (onboard ERS-2 launched 21st April 1995) with three additional channels in the visible (see table 1) allow new possibilities for land studies with high accuracy estimation and geolocation. Both sensors have two different angles of view.

Channel	λ [micron]	Range [micron]	Dynamic range	NE Δ T a	S/N a	0.5% Γ
1 - IR	12.0	11.5 ÷ 12.5	200 ÷ 318 K	0.05 K		
2 - IR	10.9	10.4 ÷ 11.3	200 ÷ 321 K	0.05 K		
3 - SWIR	3.7	3.55 ÷ 3.93	0 ÷ 311 K	0.08 K		
4 - NIR	1.6	1.58 ÷ 1.64	0 ÷ 7 mW cm ⁻² μ m ⁻¹ sr ⁻¹		20:1	
5 - NIR	0.865	0.855 ÷ 0.875	0 ÷ 30 mW cm ⁻² μ m ⁻¹ sr ⁻¹		20:1	
6 - VIS	0.659	0.649 ÷ 0.669	0 ÷ 45 mW cm ⁻² μ m ⁻¹ sr ⁻¹		20:1	
7 - VIS	0.555	0.545 ÷ 0.565	0 ÷ 50 mW cm ⁻² μ m ⁻¹ sr ⁻¹		20:1	

Table 1 – Radiometric and spectral characteristic of ATSR-2 (Outline Scientific Description, ER-RS-RAL-AT-2003)

Moreover, an Advanced ATSR (AATSR) will be onboard the ESA's satellite ENVISAT (due to be launched in the 2000). This will allow to use the know-how and techniques developed for the previous ATSR until the 2006. Raw ATSR data are processed (SADIST level 1B product - Bailey 1994) giving calibrated and geolocated images of 512x512 pixels. The pixel has a resolution of 1-Km in the seven channels and the latitude and longitude is given for each pixel. Thanks to the reduced field of view across the path, a swath large 509 Km avoids edge pixels to be seen at high angle of sight. In this way the ground area associated with these pixels are close to one square area of 1Km x 1Km. The images in the Thermal and Middle Infrared (TIR & MIR) are brightness temperature at Top of

Atmosphere (TOA) digitized at 12 bits. The visible and near infrared (NIR) are converted to TOA reflectance using correction factors produced by Rutherford Appleton Laboratory (<http://www.atrs.rl.ac.uk/calibration.html>). Thanks to the ERS-2 repeat cycle (35 days) and the ATSR-2 swath (509 Km) the same point on the earth surface is observed at least every three days. This period is satisfactory enough for the study of burned surface occurrence, considering the different vegetation burning, which can show a very fast growth (e.g. savanna) or annual permanent scars on the vegetation layer (e.g. boreal forest). Another interesting feature of ATSR-2 is that the overpass time is 10:30 at the equator. At this hour the ground already shows its characteristics in terms of heat exchange, but the formation of the typical afternoon clouds due to the water surface evaporation is still negligible.

4. Methodology for automatic burned surfaces estimation

The research design adopted in the development of the methodology is represented in figure 2. In particular the main physical variations which can be detected in the remotely sensed data over a vegetation layer after the fire were identified with different methods in order to create six different images of scalar parameter. These values were identified from K1 to K6 and are more directly linked to the burned surface occurrence than the original spectral value.

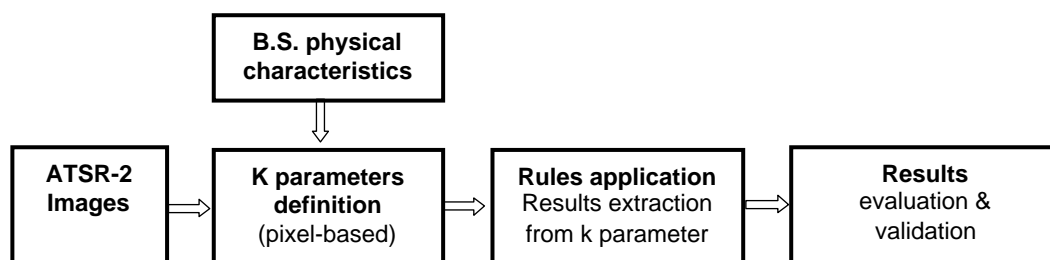


Figure 2. Research design. The concept is to transfer to k-parameter the burned surface information holds in the remotely sensed data, in order to reduce the amount of useless data to be evaluated. The final results are evaluated with different rules on the K parameters.

4.1 Physical characteristics of burned surfaces

The healthy vegetation shows higher reflectance in the range between 0,7 micron and 1,3 micron (NIR) than other natural surfaces (Tucker et Seller, 1986). In general this region of the spectrum contains the most useful information for burned surface detection, thanks to the strong reflectance variation that can be found after the fire occurrence (Pereira et Setzer 93, Pereira 99).

The second physical characteristic is the increase of temperature that occurs in a burned surface. Normally in a vegetation layer under the sun heat, the temperature maintains a normal level because energy is transferred to the atmosphere in form of latent heat through water vapor. The presence of ash and carbon constitutes a dry layer that doesn't allow this cooling process, increasing the surface temperature by 7÷8 K (Lambin et Erlich 1996). The third characteristic is based on the contextual variability visible between burned and normal vegetation surfaces in the red channel. Normally the values detected at this wavelength for different ground coverages show very low variation, but in presence of burned surfaces, the standard deviation increases for the reflectance detected in the red. This feature is the less "burn-related" than the other, but the information given by this behavior has been investigated.

4.2 K-parameters definition

The definitions of the scalar parameters are based on the three physical characteristics identified over the burned surfaces.

Using the different evaluation approach based on spectral/temporal/spatial variations, the six scalar values were defined (table 2), directly linked to the burned surface occurrence on the pixel under analysis.

Spectral-based parameters

- K1: identified in the 0.87/11 micron scatterplot
- K2: decrease on GEMI where 3.7 is saturated
- K3: identified in the 12/11 micron scatterplot

Time-based parameters

- K4: low 0.87 reflectance after the fire events
- K5: high 11 BT after the fire events

Spatial/time-based parameter

- K6: high std on 0.67 micron 3x3 grid

4.2.1 K1 parameter

Plotting the graph between reflectance in the NIR (0.87 micron) and brightness temperature in the TIR (11.0 micron), it is possible to identify a geometrical behavior of the point associated with pixels of burned surface. The

point associated with burned surface moves away from the overall distribution, in the upper left direction, independently from the vegetation type or atmospheric status. However these daily differences determine a variation in the total distribution of the scatterplot and must be taken into account when defining any estimation threshold. For this reason, we define a scalar parameter, directly linked to the fine or strong appearance of burned surfaces, and adaptively decorrelated from the possible daily variation (atmospheric, solar illumination etc). In particular the K1 parameter is proportional to the geometrical distance calculated in the previous scatterplot, from the point analyzed and the point defined from the mean value of both the axes. In order to optimize the method, only the points with NIR reflectance less than the mean and brightness temperature higher than the mean are considered, adjusting the final scalar value taking into account the variance in both the channel for the entire image under analysis.

4.2.2 K2 parameter

Different studies have demonstrated that the Global Environment Monitoring Index (GEMI, Pinty et Verstraete 1991) is more useful for burn scars analysis than NDVI or other classical vegetation indexes (Pereira 1999, Chuvieco 1999). The second parameter (K2) is defined as the difference between the mean GEMI value in an image and the GEMI value on the considered pixel. For the K2 image definition, only the pixels that show a brightness temperature at 3,7 micron higher than 312 K ($BT_{3,7} > 312K$) are considered, in order to mask water bodies, with low GEMI values too.

4.2.3 K3 parameter

For this third parameter only the thermal property of a burned surface was used. Considering the scatterplot made with the data at 11 micron and 12 micron, the K3 was set equal to the distance from the point identified with the mean values and the pixel value, always taking into account the variance of the entire image for better discrimination.

4.2.4 K4, K5 parameters

The percentage difference between the NIR value and the mean NIR value in the image was used to create the K4 parameter's image. This simple procedure has been applied to store images that had been used in a further temporal analysis, defined in the application rules phase. Using the same concept the K5 was defined like the difference between brightness temperature at 11 micron and the mean value for the entire image in the same channel.

4.2.5 K6 parameter

The last parameter was defined from the spatial feature identified over burn. The K6 array represents the variance calculated in the RED channel for each 3x3 grid centered in the pixel under analysis.

4.3 Rules definition

The rules allow to obtain different burned/unburned estimations from the six K parameters already defined. A bayesian method was used in order to decorrelate the final estimation from different vegetation types. In particular K1 K2 and K3 data are also calculated from a training set of burned surfaces of the same vegetation under analysis and the results were used in the bayesian estimator, evaluating the probability $P(BS/Kval)$ that the pixel belong to burned surface if his K value is at certain level, using the formula:

$$P(BS/Kval)=P(Kval/BS)*P(BS)/P(Kval)$$

Where:

$P(BS/Kval)$ is the probability that a pixel is burned if its value is Kval;

$P(Kval/BS)$ is the probability that occurs a certain K value over a burned surface zone (calculated on the training set images);

$P(Kval)$ is the probability that a K value occurs (calculated on the training set images);

$P(BS)$ is the "a priori" probability to obtain a certain amount of burned surface in the image under analysis (set to a neutral value of one if there aren't any "a priori" assumption).

From the probability calculation of the first three parameters, a threshold has been defined for these values in order to discriminate the burned/unburned pixels.

These thresholds were set to optimize the estimation on the training set images.

A temporal approach has been used to define the rules for K4, K5 and K6 parameters. Considering the time series value for each of these parameters on the same pixels, in order to obtain a temporal behavior filtered from error caused by cloud cover or great daily variations, the time series were averaged with a temporal window of six-sample length. The resulting time series appear smoothed, but show clearly the temporal variations connected with new

burned surfaces occurrence. In particular a decrease in the K4 time series or an increase in the K5 or K6 time series is associated with a permanent variation on the ground, mainly because the vegetation has been burned. So, if the decrease/increase in these time series exceeds a threshold based on the mean time series values, the correspondent pixel is identified as burned surfaces.

5. Validation and discussion

The different procedures were tested on the identified area and validated using nine Landsat Thematic Mapper (TM) images, located on different vegetation zones and for different days (figure 3).

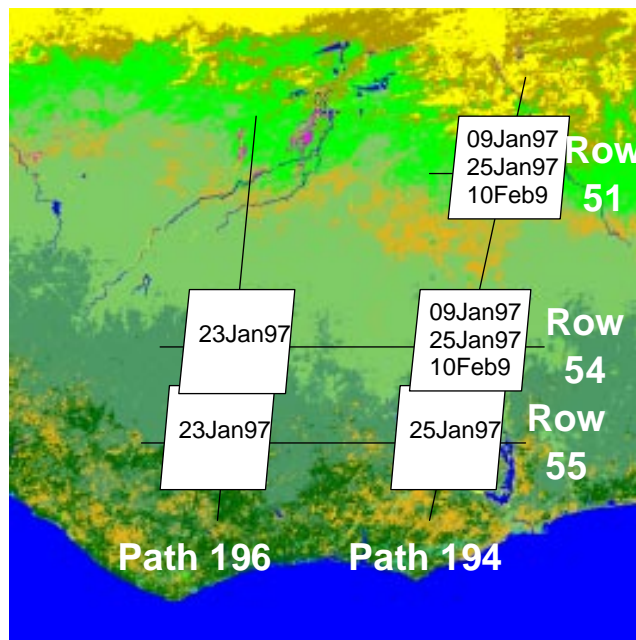


Figure 3. Multi-temporal Landsat TM coverage over IGBP Land cover classification, in the area under analysis.

The high-resolution data were sub-sampled at 125 meters resolution, in order to allow a more direct comparison with low-resolution estimation from ATSR-2 data, without loss of useful information. By this way, for each low-resolution pixel (1 Km) in the K parameter or vegetation map, a grid of 8x8 high-resolution pixels (125 meters), called SC/TM (Supervised Classification from TM) is available. The burned surface area was estimated by supervised classification, with the maximum likelihood method. In particular five different classes were identified in the images (burned surfaces, vegetation, river, clouds and cloud's shadows) and their spectral signatures in the seven TM channels were collected from a sample set identified by visual inspection. All the available images were georeferenced in order to make a multi-layer database, containing six estimation from the K parameter, the vegetation map (IGBP 1996) of Africa and the supervised classification from Landsat. The results of the supervised classification describe a different occurrence of burned surface in the nine images under analysis which can be summarized in two different classes:

- Areas where the burned surfaces are sparsely and present different extension:
- Areas with very high occurrence of burned surfaces and low percentage area of healthy vegetation.

Since the estimation algorithms identified were defined making use of large areas (50x30 Km), containing a large percentage of healthy vegetation to allow the calculation of mean normal value, if the majority of the image is burned, omission errors will increase. This aspect was taken into account in the validation. However in order to solve this problem we used normal mean value for the vegetation, that arise from a larger area or archive data based on the same biomes under analysis.

By comparing the available data in different ways (Kpar, VEG, SC/TM) it is possible to obtain the four following validation results.

A. Comparison between SC/TM and Kpar.

To compare the amount of area estimated from the different K parameter with the supervised classification from TM data, taking into account the different sensor's resolution and geolocation problems, a set of sub-area was identified around burn scars occurrence in the supervised classified images. Inside each sub-area, the burned surfaces in square kilometers was calculated with the estimation derived from each K parameters and from the supervised classification. Performing a regression analysis (figure 4) on the retrieved areas, on sparsely burned occurrence areas, the regression coefficient from K1 and K3 estimator are near to one ($m_{K1}=1.03$, $m_{K3}=1.11$) and the offsets are also very low.

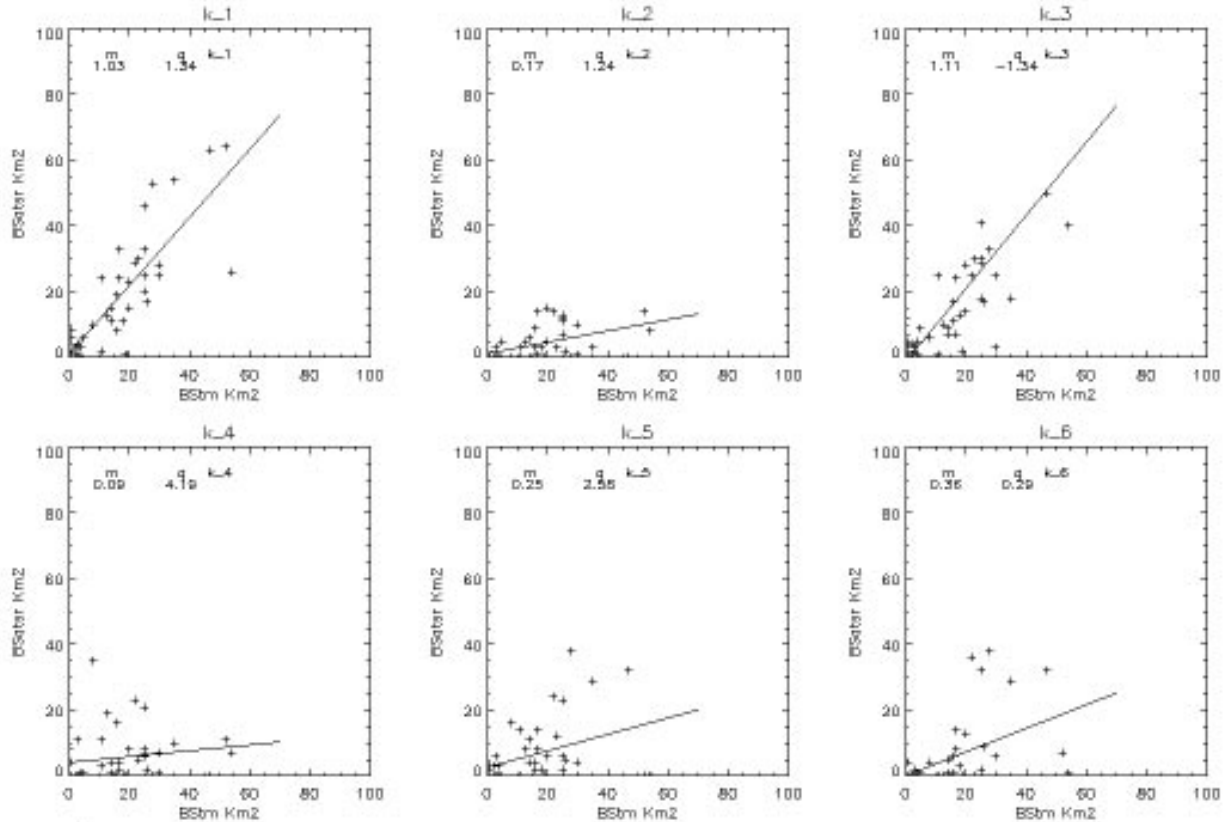


Figure 4. Regression analysis between the B.S. area estimated from K-parameter and from Landsat supervised classification (zone with sparsely burned surface occurrence). In the graphs are also represented the regression coefficient m and the offset q .

Moreover in a pixel-based validation it is possible to highlight the accuracy of the different K parameter methods with respect to the sub-pixel occurrence of burned surface. Considering only zones with sparsely B.S. and plotting the number of pixels estimated from Kpar (1 Km res) versus the percentage of burned inside each pixel (from SC/TM 125 mt res) it is possible to obtain the graphs in figure 5. Up to 30% of the pixels estimated from K1 are burned for more than 80%. This value increases with the proportion of area burned inside the single pixel. For the area with high occurrence of burned surfaces, although the methods are defined in area with sparsely burn scars, the number of pixels estimated from K1 and K3 increase with the burned sub-pixel proportion (figure 5). This means that on these particular areas, only the pixels with very high characteristics of B.S. are recognized, confirming the accuracy of the method. This omission error can be eliminated using values of healthy vegetation not obtained from a 50x30 Km area (improvement under investigation).

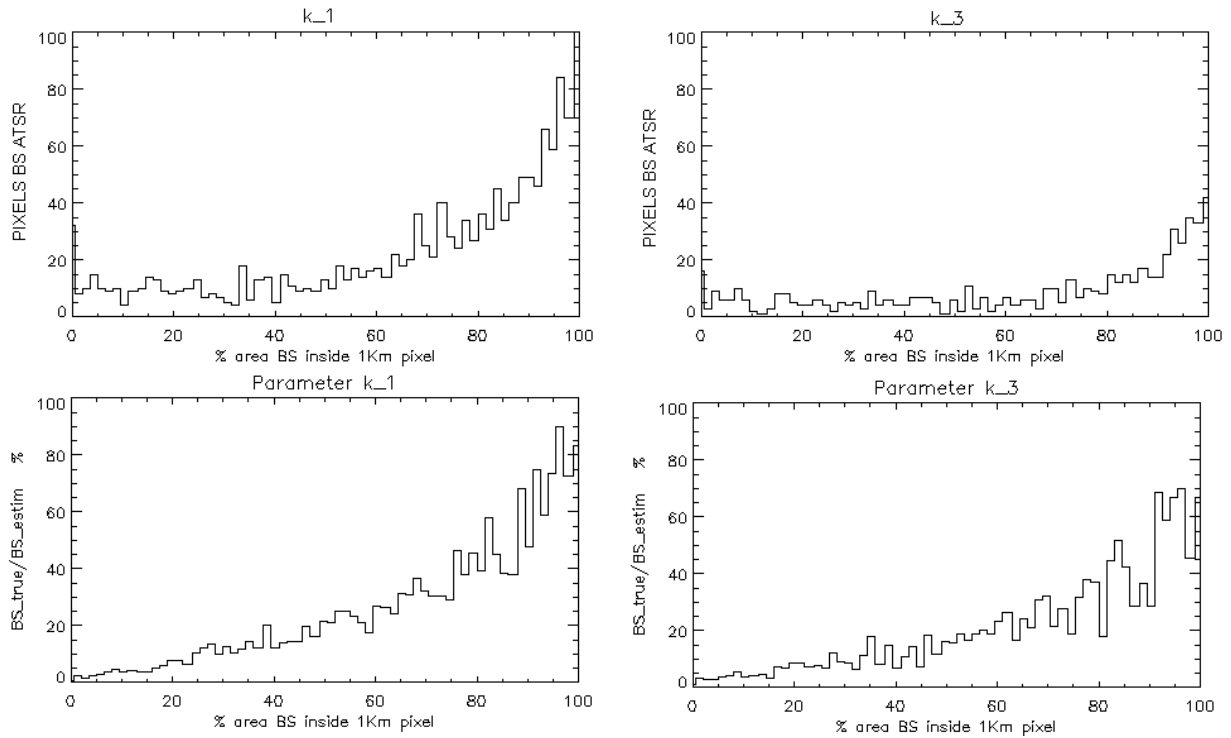


Figure 5. Evaluation of the K1 and K3 estimation on the sub-pixel analysis. The first two graphs represent the number of pixels estimated like B.S. versus the percentage of B.S. inside the single low-resolution pixel. The last two graphs show the accuracy of the estimation when applied in area with high burned surface occurrence.

B. Burned surface from SC/TM and vegetation types

The distribution of the burned surface in the different vegetation area were calculated with the TM results (table 3). The results show that in the area under analysis 20.72% of woody savanna and 20.86% of savanna were burned, against only 2.73% on evergreen broadleaf forest. These results are validated by previous studies (Hao et Liou 1994), confirming a good accuracy in the supervised classification on the TM, used for the K parameter validation.

Vegetation type	Total area [Km ²]	Total B.S. [Km ²]	B.S. %
Evergreen broadleaf forest	5632	153.73	2.73
Woody savanna	30101	6236.28	20.72
Savanna	49923	10414.22	20.86
Grassland	2587	117.39	4.54
Cropland & natural vegetation mosaic	17181	911.94	5.31

Table 3. Proportion of burned surface contained in each vegetation types under analysis, estimated with supervised classification on Landsat TM images.

C. K-parameters and vegetation cover

In order to evaluate if the K methods see burned surfaces over a particular vegetation cover, we compared the percentage of burned surface estimated in each vegetation with the percentage of presence of that vegetation type. From the figure 6 it is possible to note that woody savanna cover 28% of the area under analysis, but the K1 estimation gives 39% in woody savanna. From previous analysis we know that 34% of woody savanna was burned, so K1 seems to overestimate the result. Moreover only in this vegetation cover the K1 result is higher than the vegetation presence. The same behavior occurs for K2 and K4 in savanna, K3 on Cropland and for K5 and K6 on woody savanna. These results show in which vegetation cover the different k-parameters estimate the majority of burned surface, but the validation should include the analysis using the SC/TM.

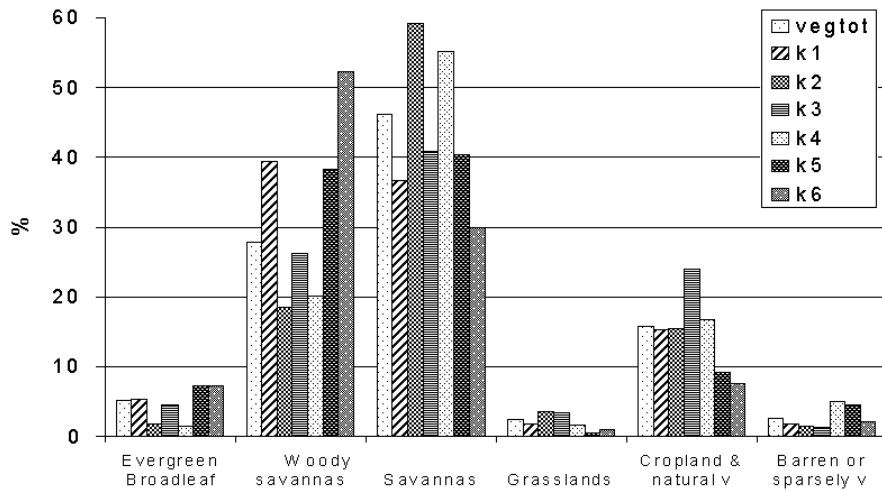


Figure 6. K estimation percentage for different vegetation covers. The first level on the left for each vegetation group is the vegetation percentage in the area under analysis. The other six bars are the b.s. percentage of the correspondent K parameter retrieved in the vegetation type considered.

D. K parameters versus SC/TM for different vegetation cover.

By comparing the surface estimated by each parameter in different vegetation cover with the estimation from SC/TM, it is possible to evaluate the estimation accuracy in different vegetation for each parameter (figure 7). The results show a good behavior of K1 on evergreen broadleaf forest, savanna and cropland (accuracy near to 100%) and for K3 in evergreen broadleaf forest and cropland (accuracy near to 100%). A very different behavior in woody savanna arises for K1, that overestimates the b.s. and K3 that underestimates it. The other parameters seem to always underestimate, except K5 and K6 in woody savanna which achieve accuracy up to 70%.

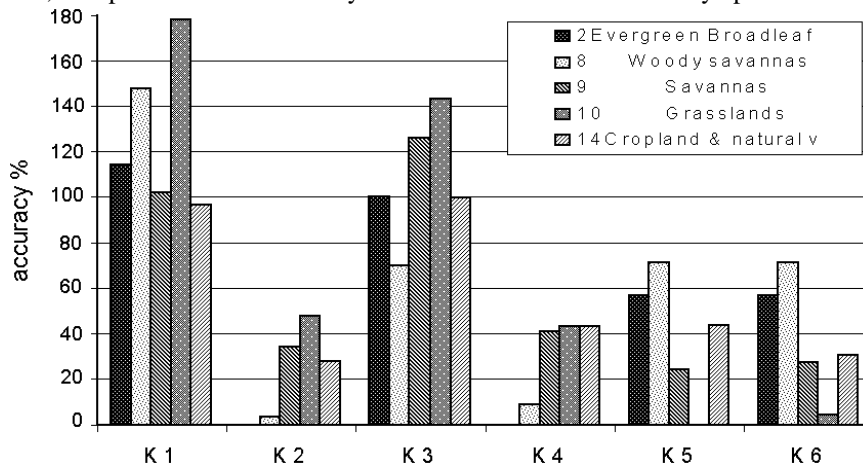


Figure 6. Accuracy estimation for each K parameter in different vegetation covers.

All these results, in particular from the D. validation will be used for the definition of a final parameter, able to estimate the burned surfaces over all the vegetation cover, taking into account the information given by all the six parameters already tested.

Conclusion

A new adaptive method has been developed and tested on a large number of ecosystems ranging from latitude 15°N to 6°N in Africa. This method has been applied to ATSR-2 data, which turned out to be well suited to this study, due to the good radiometry and geometry of the instrument. The first validation results indicate further improvements. The perspective is to derive an harmonized global method simple enough to run on 1 Km global data set for several consecutive years.

This method, together with other developed at EU/JRC and University of Lisbon will be tested in different continents in order to achieve a common global algorithm. This exercise is part of the ERS-AO3 as AO-329.

References

- ARINO, O., MELINOTTE, J.M., 1995. Fire Index Atlas, *Earth Observation Quartely*. n°50, 11-16 December 1995. *ESA Publications*.
- CHUVIECO E., MARTIN P. 1999. TN 132-10 Forest Fire Earth Watch. Performance Assessment in the post-fire phase.
- HAO, W.M., and LIU, M.H., 1994. Spatial and temporal distribution of tropical biomass burning. *Global biogeochemical cycles*. Vol. 8 n°4 495-503.
- IGBP 1996. Newsletter n.27 September 1996.
- KASISCHKE, E.S., and FRENCH, N.H.F., 1995. Locating and estimating the area extent of wildfires in Alaskan boreal forest using multiple-season AVHRR NDVI composite data. *Remote sensing of the environment*. **51**, 263-275.
- LAMBIN, E.F., ERLICH, D. 1996. The surface temperature-vegetation index space for land cover and land cover change analysis. *International Journal of Remote Sensing*. **17**, 463-487.
- LEVINE, 1991, Global Biomass Burning: Atmospheric, Climatic and Biosphere Implication, *Global Biomass Burning, Atmospheric, Climatic and Biospheric Implication*. Edited by J.S.Levine. **Intr.**
- LIOUSSE, C., DULAC, F., CACHIER, H., TANRE', D., 1997. Remote Sensing of Carbonaceous Aerosol Production by African Savanna Biomass Burning. *Journal of Geophysical Research*., **102(D5)** 5895-5911.
- PEREIRA, M.C., SETZER, A.W., 1993. Spectral characteristics of deforestation fires in NOAA/AVHRR images. *International Journal of Remote Sensing*, **14**, 583-597.
- PEREIRA, M.C., SETZER, A.W., 1996. Comparison of fire detection in savannas using AVHRR's channel 3 and TM images. *International Journal of Remote Sensing*, **17**, 1925-1937.
- PEREIRA, M.C. 1999. A comparative evaluation of NOAA/AVHRR vegetation indexes for burned surface detection and mapping. *IEEE Transaction on geoscience and remote sensing*., **37**, 217-226.
- PINTY, B., VERSTRAETE, M.M., 1991. GEMI: A Non Linear Index to Monitor Global Vegetation from Satellites, *Vegetation* 101, 15-20.
- RAZAFIMPANILO, H., FROUIN, R., IACOBELLIS, S.F., SOMMERVILLE, R.C.J. 1995. Methodology for Estimating Burned Area from AVHRR Reflectance Data. *Remote sensing of the environment*. **54**,273-289.
- BAILEY, P., 1994. SADIST Products (version 600) Space Science Department – Rutherford Appleton Laboratory. 25 May 1994
- SEILER, A. W., e CRUTZEN P.J., 1980, Estimates of grass and net fluxes of Carbon Between the Biosphere and the Atmosphere from Biomass Burning. *Climate Change*. **2** 207-247
- STRICKER, N. C. M., HAHNE A., SMITH D.L., DELDERFIELD J., OLIVIER M.B., EDWARDS T. 1995. ATSR-2 The evolution in its design from ERS-1 to ERS-2. *ESA Bulletin Number 83*, August 1995.
- TUCKER, C. J., SELLERS, P.J., 1986 Satellite remote sensing of primary products. *International Journal of Remote Sensing*, **7**, 1395-1416.